Time-dependent wave packet and quasiclassical trajectory study of the $C(^3P)+OH(X\,^2\Pi)\rightarrow CO(X\,^1\Sigma^+)+H(^2S)$ reaction at the state-to-state level

Niyazi Bulut,[1] Alexandre Zanchet,[2,a)] Pascal Honvault,[3,b)] Béatrice Bussery-Honvault,[3] and Luis Bañares[4]
[1]*Department of Physics, Firat University, 23169 Elaziğ, Turkey*
[2]*Institut de Physique de Rennes, UMR CNRS 6251, University Rennes 1, 35042 Rennes Cedex, France*
[3]*Institut UTINAM, UMR CNRS 6213, University of Franche-Comté, UFR Science et Techniques, 25030 Besancon Cedex, France*
[4]*Departamento de Química Física, Facultad de Química, Universidad Complutense, 28040 Madrid, Spain*

(Received 21 January 2009; accepted 7 April 2009; published online 19 May 2009)

The first calculations of state-to-state reaction probabilities and product state-resolved integral cross sections at selected collision energies (0.05, 0.1, 0.5, and 1.0 eV) for the title reaction on the *ab initio* potential energy surface of [Zanchet *et al.* J. Phys. Chem. A **110**, 12017 (2006)] with the OH reagent in selected rovibrational states ($v=0-2$, $j=0-5$) have been carried out by means of the real wave packet (RWP) and quasiclassical trajectory (QCT) methods. State-selected total reaction probabilities have been calculated for total angular momentum $J=0$ in a broad range of collision energies. Integral cross sections and state-specific rate coefficients have been obtained from the corresponding $J=0$ RWP reaction probabilities for initially selected rovibrational states by means of a capture model. The calculated RWP and QCT state-selected rate coefficients are practically temperature independent. Both RWP and QCT reaction probabilities, integral cross sections, and rate coefficients are almost independent of the initial rotational excitation. The RWP results are found to be in an overall good agreement with the corresponding QCT results. The present results have been compared with earlier wave packet calculations carried out on the same potential energy surface. © *2009 American Institute of Physics*. [DOI: 10.1063/1.3125956]

I. INTRODUCTION

The interaction between open-shell C atoms and OH radicals is considered to be of some importance in the production of carbon monoxide in various chemical environments and plays a crucial role in astrophysics and interstellar clouds.[1–4] Quantum mechanical (QM) reactive scattering studies of reactions involving such open-shell species require high level global three-dimensional *ab initio* potential energy surfaces (PESs). This type of reaction usually involves a PES characterized by a deep potential well and the presence of two heavy atoms, which makes QM calculations very challenging since many channels have to be considered to get well converged results.[3]

The first global *ab initio* PES for the $C(^3P)+OH(X\,^2\Pi)$ reaction was recently built by Zanchet *et al.*.[1] This PES is based on more than 2000 *ab initio* points computed at the multireference (MR) internally contracted single and double configuration interaction level plus Davidson correction using Dunning's aug-cc-pVQZ basis sets.[1] The MR space was taken to be a complete active space. The *ab initio* points were fitted using the reproducing kernel Hilbert space methodology. It was found that the $C(^3P)+OH(X\,^2\Pi)\rightarrow CO(X\,^1\Sigma^+)+H(^2S)$ reaction is highly exothermic (≈6.4 eV) and barrierless relative to the entrance channel, while three minima and five potential barriers were located on the surface. The three minima correspond to the formation of HCO and COH complexes and to the CO+H products, with the COH complex being a metastable minimum relative to the product channel. The five saddle points correspond to potential barriers for both the dissociation/formation of HCO and COH into/from CO+H, to barriers for the isomerization of HCO into COH, and to barriers for the inversion of HCO and COH through their respective linear configurations.

The first theoretical cross sections and rate coefficients on this PES were calculated by Zanchet *et al.* employing the quasiclassical trajectory (QCT) method.[2] In that work, total and state-specific integral cross sections were calculated as a function of collision energy. The calculated thermal rate coefficients were found to be practically temperature independent at high enough temperatures and almost invariant on the rovibrational state of the OH reagent. Employing this same PES, Zanchet *et al.*[3] performed new QCT calculations to obtain differential cross sections (DCSs) and product energy distributions in a wide range of collision energies and to explore the influence of the reagent diatom rovibrational excitation on these quantities. It was found that rovibrational excitation of OH has no effect on the product vibrational, rotational, and translational distributions, but DCSs show a weak dependency on the initial rotational state of the reagent molecule. An analysis of the results was performed in terms of the lifetimes of the intermediate complexes and on the kinematic constraints associated with the mass combination.

Following these QCT studies, Lin *et al.* performed the

a)Present address: Instituto de Fisica Fundamental (CSIC), Serrano 123, E-28006 Madrid, Spain.
b)Author to whom correspondence should be addressed. Electronic mail: pascal.honvault@univ-fcomte.fr.

first exact wave packet (WP) calculations for $J=0$ using a flux analysis method on the same PES.[4] Calculations were carried out using reactant Jacobi coordinates. In those calculations, the main objective was to compute the total reaction probability as a function of collision energy without resolving the final quantum states of the products. It was found that the title reaction is almost completely dominated by the capture of the reactants and thus calculations at $J \geq 0$ were carried out using a capture model. The reported integral cross sections and rate coefficients were found to be in good agreement with the earlier QCT results except at low collision energies and low temperatures, respectively.

In the present work, we have applied the real wave packet (RWP) method originally developed by Gray and Balint-Kurti[5] and the QCT method to study the title reaction on the PES of Zanchet *et al.*[1] at the state-to-state level. WP calculations have been carried out using product Jacobi coordinates at zero total angular momentum, $J=0$, and we have been able to obtain state-to-state reaction probabilities. State-to-state integral cross sections have been computed using a capture model,[6] which has been proved to be an excellent approximation for total (not state-resolved) integral cross sections for the title reaction.[4] The corresponding state-selected rate coefficients have been calculated by Boltzmann averaging of the integral cross sections. The RWP results have been thoroughly compared with QCT calculations on the same PES.

The organization of the paper is as follows: In Sec. II we will briefly review the RWP and QCT theoretical methods employed in this work, Sec. III will present the results and discussion, and finally Sec. IV will close with the conclusions.

II. THEORY

A. Real wave packet method

The method used for the calculations presented here is the RWP approach by Gray and Balint-Kurti.[5] The RWP method has been well documented in the literature[5,7,8] and only the details relevant to the present work will be given here.

The basic idea of the RWP approach is to map the Hamiltonian operator as[5]

$$f(\hat{H}) = -\frac{\hbar}{\tau}\cos^{-1}(\hat{H}_s), \tag{1}$$

where $\hat{H}_s = a_s\hat{H} + b_s$ with a_s and b_s chosen to ensure that the minimum and maximum eigenvalues of $\hat{H}_s$ lie in the interval $(-1,1)$. The WP then evolves under the modified time-dependent Schrödinger equation

$$i\hbar\frac{\partial\Psi(x,t)}{\partial t} = f(\hat{H})\Psi(x,t), \tag{2}$$

where x donates all coordinates. The functional mapping of the Hamiltonian operator allows the propagation of the WP to be achieved by a Chebyshev iterative method where each step requires a single evaluation of the action of the Hamiltonian on the real part of the WP. This approach shares many features with the work of Huang *et al.*,[9,10] Mandelshtam and Taylor,[11,12] Kroes and Neuhauser,[13] Chen and Guo,[14] and Althorpe.[15]

TABLE I. Parameters used in the RWP calculations (all parameters are given in a.u.).

Reactant scattering coordinate range	$R_{min}=0.1$, $R_{max}=18.0$
Number of grid points in R	255
Diatomic coordinate range	$r_{min}=0.7$, $r_{max}=18.0$
Number of grid points in r	479
Number of angular basis functions	100
Center of initial WP	$R_0=14.5$
Gaussian width factor	$\alpha=20.5$
Initial translational kinetic energy (eV)	$k_0=0.4$
Analysis point	10.0
Number of Chebyshev iterations	70 000

The propagation of the WP may be carried out in terms of either in a reactant Jacobi coordinate system or in a product Jacobi coordinate system. In the present calculations the propagation grid scheme is defined using the product Jacobi coordinates so as to permit the computation of state-to-state reaction probabilities. The initial WP is first expressed in reactant Jacobi coordinates and then transformed to product Jacobi coordinates before the propagation started. The wave function is propagated in these coordinates and analyzed at a line located in the asymptotic region of the product channel. The calculations require 70 000 iteration steps to get converged results. The final WP is analyzed to extract the $\underline{S}$ matrix elements for the lowest 40 vibrational and 100 rotational states. The initial conditions used in all the calculations set the initial state of the reactants to $(v, j) = (0-2, 0-5)$. In order to calculate the reaction probabilities for each initial rovibrational state it is necessary to integrate separately the initial WP for each rovibrational state v, j of the reagent molecule. The calculations are carried out with the same parameters for each initial rovibrational state in a broad range of collision energies. All grid parameters used in the calculations are given in Table I.

The calculation of the integral cross sections as a function of collision energy for each rovibrational state v, j of the reagent molecule requires summing up all the partial waves as follows:

$$\sigma_{vj}(E_c) = \frac{\pi}{k^2}\frac{1}{2j+1}\sum_{J=0}^{J_{max}}(2J+1)P_{vj}^{J}(E_c), \tag{3}$$

where k is the modulus of the wave-number vector, $k^2 = 2\mu_r E_c/\hbar^2$, μ_r is the reduced mass of the system, and E_c is the collision energy.

In the original presentation of the capture model,[6] total reaction probabilities out of specific v, j initial states were employed and the corresponding total reaction cross sections were estimated. As noted by Hankel *et al.*,[16] here we assume that the capture model can be applied to the calculation of integral cross sections associated with different rovibrational states of the reagents and the various final (CO) vibrational states v'. It is expected that such a model is most accurate for the least state-resolved quantities and, thus, we did not attempt to use this approach to obtain v', j' specific integral

cross sections but rather concentrated on v' state-resolved cross sections summed over all final j' states.

For barrierless reactions, one of the simplest approximations to calculate reaction probabilities for $J>0$ is the capture model as proposed by Gray *et al.*[6] Within this model, it is assumed that the dynamics is dominated by an effective potential which exhibits centrifugal barriers as a function of J. These barriers are assumed to replace the role of the J-shifting barrier. This model is computationally much less demanding than the accurate quantum dynamic scattering calculations for $J\neq 0$. In this approximation, initial v, j state-selected total reaction probabilities for $J>0$ are calculated by using

$$P_{vj}^{J}(E_c) = P_{vj}^{J=0}[E_c - E_{\text{shift}}^{J}], \tag{4}$$

where $P_{vj}^{J=0}$ is the initial v, j quantum state-resolved reaction probability for $J=0$ as a function of translational energy E_c and $P_{vj}^{J}(E_c)$ is the estimated reaction probability for a higher value of J at energy $E_c - E_{\text{shift}}^{J}$. The shifting energy E_{shift}^{J} is the barrier associated with an effective potential that can be defined as

$$E_{\text{shift}}^{J}(R) = \langle vj|V|vj\rangle + \frac{\hbar^2}{2\mu_r R^2} J(J+1), \tag{5}$$

where R is the distance between the atom and the center of mass of the reagent molecule.

The v, j initial state-selected rate coefficient is calculated by averaging the corresponding integral cross section $\sigma_{vj}(E_c)$ over translational energy as

$$k_{vj}(T) = \frac{1}{Q_{\text{el}}}\left(\frac{8}{\pi\mu_r (k_B T)^3}\right)^{1/2} \int_0^\infty E_c \sigma_{vj}(E_c) e^{-E_c/k_B T} dE_c, \tag{6}$$

where k_B is the Boltzmann constant, E_c is the translational energy, and Q_{el} is the electronic partition function. For the title reaction, the electronic partition function is given by[2]

$$Q_{\text{el}} = \frac{g_0^{\text{C}} + g_1^{\text{C}} e^{-\Delta E_1/T} + g_2^{\text{C}} e^{-\Delta E_2/T}}{g^{\text{COH}}} \times [g_{1/2}^{\text{OH}} + g_{3/2}^{\text{OH}} e^{-\Delta E_3/T}], \tag{7}$$

where the first term is related to the carbon atom; $\Delta E_1(^3P_0 - {}^3P_1) = 23.6$ K and $\Delta E_2(^3P_1 - {}^3P_2) = 62.6$ K are the energy splittings between the fine structure sublevels of the ground ^3P state and the factors $g_0^{\text{C}}=1$, $g_1^{\text{C}}=3$, and $g_2^{\text{C}}=5$ refer to their electronic degeneracy. $g^{\text{COH}}=2$ is the degeneracy of the COH ground state. The second term is related to the OH radical where $\Delta E_3 = 205$ K represents the energy splitting $^2\Pi_{1/2} - {}^2\Pi_{3/2}$ and $g_{1/2}^{\text{OH}} = g_{3/2}^{\text{OH}} = 2$ as each of these two states is doubly degenerate. This equation shows that the electronic partition function goes asymptotically to 18 for high temperatures where the 18 PESs are accessible while only 1 is reactive [that leading to the $\text{CO}(X\,^1\Sigma^+) + \text{H}(^2S)$ products] and is close to 1 at very low temperatures where only the lowest reactive surface is accessible.

The thermal rate coefficient is obtained from the state-selected rate coefficients, $k_{vj}(T)$, as follows:

$$k(T) = \sum_{v,j} \frac{(2j+1)e^{-E_{vj}/k_B T}}{Q_{vj}} k_{vj}(T), \tag{8}$$

where E_{vj} is the rovibrational energy for the v, j rovibrational state of OH and Q_{vj} is the corresponding rovibrational partition function.

B. Quasiclassical trajectory calculations

The QCT code developed by Halvick and Rayez[17] has been used for the calculation of reaction probabilities, cross sections, and rate coefficients. As the QCT method has been well documented in previous works,[1–3] we summarize here only the most relevant details for the present study.

The QCT calculations employed a standard Monte Carlo sampling of the initial conditions and the step adaptive Adams method has been used to integrate the set of Hamilton equations. We have carefully checked the conservation of both the total energy and angular momentum. At each integration step, a relative precision of 10^{-8} for the distances and for the momenta has been required. This yields to a conservation of total energy and total angular momentum with an average error of 10^{-4} eV and $10^{-5}\hbar$ respectively. A batch of 20 000 trajectories computed with a relative error of 10^{-9} has shown a change of only 10^{-2} Å^2 of the integral cross section compared to the same calculation with a relative error of 10^{-8}. The high number of trajectories ($N_t = 100\,000$) together with the high efficiency of the trajectories [(number of reactive trajectories)/$N_t = 3/5$)] gives a statistical Monte Carlo error of 0.2%. The carbon atom is initially separated from the center of mass of OH by 10 Å for the highest collision energies and 20 Å for the lowest ones. The trajectories are stopped when the recoil distance is larger than 10 Å and the recoil speed is quasiconstant. These values have been chosen in order to have negligible long range interactions. Preliminary batches of 500 trajectories were performed for each collision energy with a large maximum impact parameter. Then batches of 100 000 trajectories have been run with the appropriate value of the maximum impact parameter which varies from 9.7 to 3.2 Å as energy increases. To check the validity of the number of trajectories chosen in our study, calculations of cross sections for $\text{C}+\text{OH}(v=0,\ j=0)$ at a few translational energies have been carried out by running 200 000 trajectories in order to reduce statistical errors. The results obtained with 100 000 trajectories are coincident and quasi-identical to those obtained with 200 000 trajectories.

The quantum numbers v' and j' of the diatomic CO product have been assigned using the usual histogrammatic binning method, which consists in rounding the vibrational and rotational classical actions to the nearest integer. This procedure is one of the major shortcomings of the QCT method. However, it is essentially when the number of open rovibrational channels of the products is small that significative errors can be observed. The title reaction is hardly concerned by this drawback as long as we are only interested in the H+CO reactive channel and not in the O+CH channel. The calculations of state-to-state integral cross sections and rate coefficients have been carried out as outlined in Refs. 2 and 3.

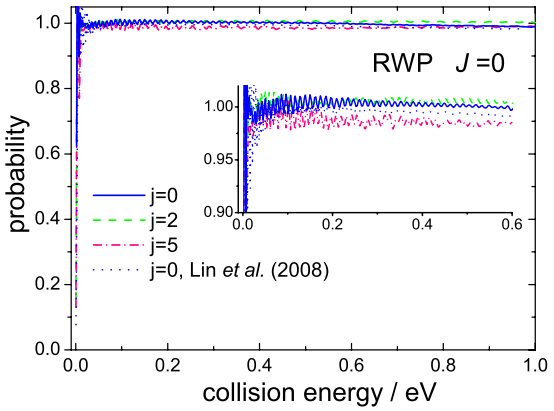

FIG. 1. (Color online) Total reaction probabilities at $J=0$ as a function of collision energy calculated using the RWP method for various initial rotational states of the OH($v=0$) radical for the title reaction. Dotted line: WP results obtained by Lin *et al.* (Ref. 4).

III. RESULTS AND DISCUSSION

A. Total and state-to-state reaction probabilities at $J=0$

The theories described above have been applied to compute total and state-to-state reaction probabilities at zero total angular momentum $J=0$ as a function of collision energy for the title reaction on the PES of Zanchet *et al.*[1]

Figure 1 shows the $J=0$ total reaction probabilities as a function of collision energy up to 1 eV calculated using the RWP method for the C+OH($v=0$, $j=0,1,2,5$) reactions. These reaction probabilities show no threshold, as expected for a barrierless reaction, reaching an average value of ≈ 1 just above 0.001 eV collision energy (steplike behavior), indicating that the nonreactive flux back to the reagents valley is essentially zero.[4] This also indicates that the reaction is dominated by the capture of the reactants because of the large exothermicity and barrierless character of the PES. Only small oscillations are observed in the low collision energy region for the various initial j, which cannot be attributed to real resonance behavior but to the incomplete damping of the outgoing WP.[4] The RWP reaction probabilities show similar magnitude and behavior for all the initial rotational states considered, demonstrating just a slight influence of OH rotational energy on reactivity. However, it is worth noticing that reactivity seems to increase first with initial j, from $j=0$ to $j=2$, and then decreases for larger j ($j=5$). The WP results for initial $j=0$ of Lin *et al.*[4] are also shown for comparison. As can be seen, the shape of the present RWP reaction probability is very similar to that of Lin *et al.*, although the magnitude of the reaction probability is somewhat larger and closer to 1 in average. This difference may be due to different convergence parameters. Or, near the reaction threshold, the damping of the slowly moving components of the WP may be incomplete in the calculations of Lin *et al.*, as already found in the O+OH case.[18]

Figure 2 depicts RWP and QCT reaction probabilities as a function of collision energy for different initial vibrational states ($v=0-2$) for initial $j=0$. The initial (v, $j=0$)-selected reaction probabilities show the same magnitude (steplike functions with probability close to 1 for collision energies larger than ≈ 0.2 eV. However, the RWP reactivity decreases as v increases for collision energies <0.2 eV. Interestingly, the oscillatory structure in the low collision energy region is more marked as the OH vibrational state goes from $v=0$ to $v=2$. The QCT reaction probabilities reproduce the overall shape of the RWP results with the exception of the low collision energy region for $v=1$ and $v=2$.

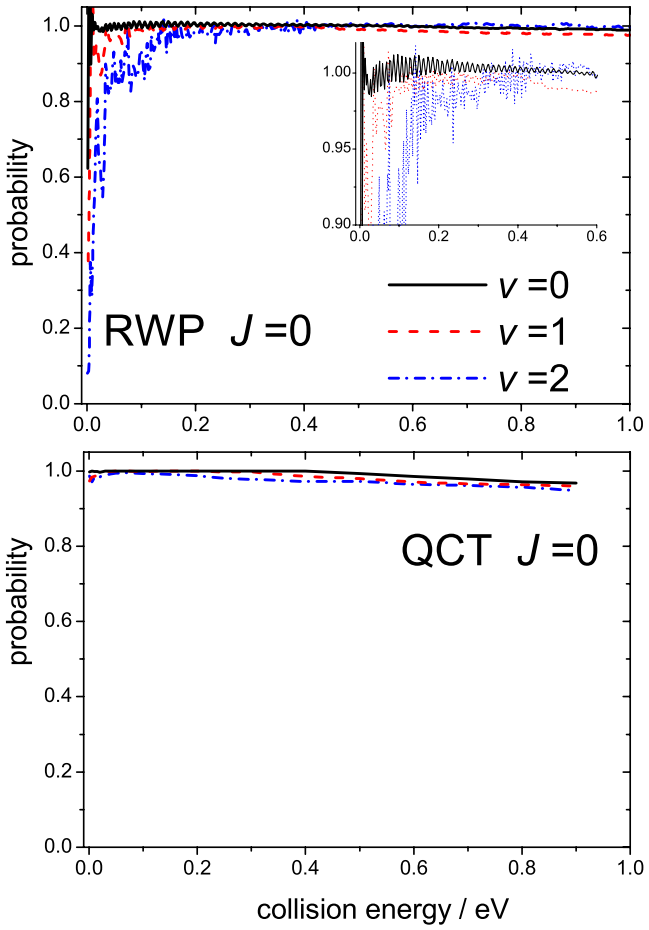

FIG. 2. (Color online) Total reaction probabilities at $J=0$ as a function of collision energy calculated using the RWP (top panel) and QCT (bottom panel) methods for various initial vibrational states of the OH radical for the title reaction.

In Fig. 3, RWP and QCT reaction probability product vibrational distributions at $J=0$ for the C+OH($v=0$, $j=0$) $\rightarrow$CO(v')+H reaction are compared at selected collision energies (0.05, 0.1, 0.5, 1.0 eV). In all cases, a substantial product vibrational excitation is observed with a clear population inversion. The RWP vibrational distribution calculated at $E_c=0.05$ eV is smooth and peaks at $v'=12-13$. In contrast, the QCT distribution is bimodal, peaking at $v'=12$ and $v'=17$ and appears to be somewhat hotter, although the maximum v' value in the distribution is similar in both RWP and QCT calculations. As collision energy increases, the RWP vibrational distributions are hotter, becoming wider and peaking at higher v' values ($v'=13-14$ at $E_c=0.1$ eV, $v'=13-14$ at $E_c=0.5$ eV, and $v'=17$ at $E_c=1.0$ eV). The QCT vibrational distributions reproduce the overall shape of the RWP distributions but show bimodal behavior at every collision energy.

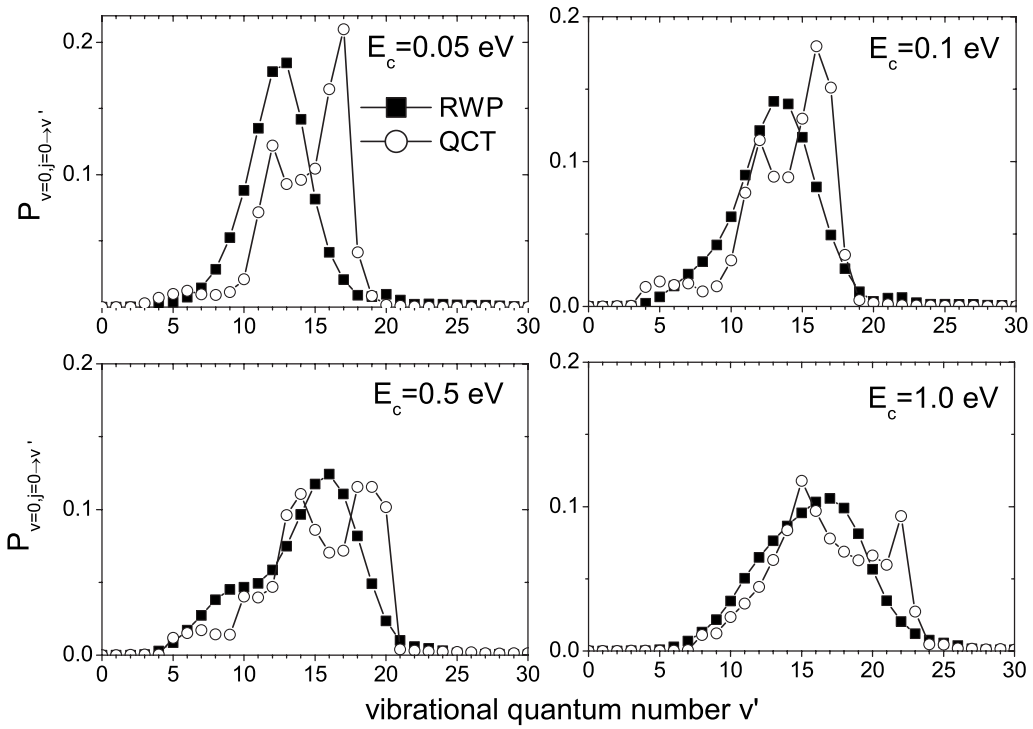

FIG. 3. Final v' state-resolved reaction probabilities at $J=0$ for the C+OH($v=0$, $j=0$)→CO(v')+H reaction at selected collision energies (0.05, 0.1, 0.5, 1.0 eV) obtained with the RWP (black squares) and QCT (open circles) methodologies.

RWP and QCT $J=0$ reaction probability vibrational distributions calculated for the C+OH($v=0-2$, $j=0$)→CO(v')+H reactions at the various collision energies (0.05, 0.1, 0.5, 1.0 eV) are depicted in Fig. 4. The main feature of the RWP vibrational distributions for the reaction with initial $v=1$ and $v=2$ is that as v increases the distributions become somewhat hotter and wider in comparison with those for the reaction with initial $v=0$. Interestingly, for the reaction with vibrationally excited OH, RWP bimodal vibrational distributions are obtained. The corresponding QCT vibrational distributions for initial $v=1$ and $v=2$ are in overall good agreement with the corresponding RWP ones.

To understand this bimodal behavior of vibrational distribution, classical trajectories have been studied in more de-

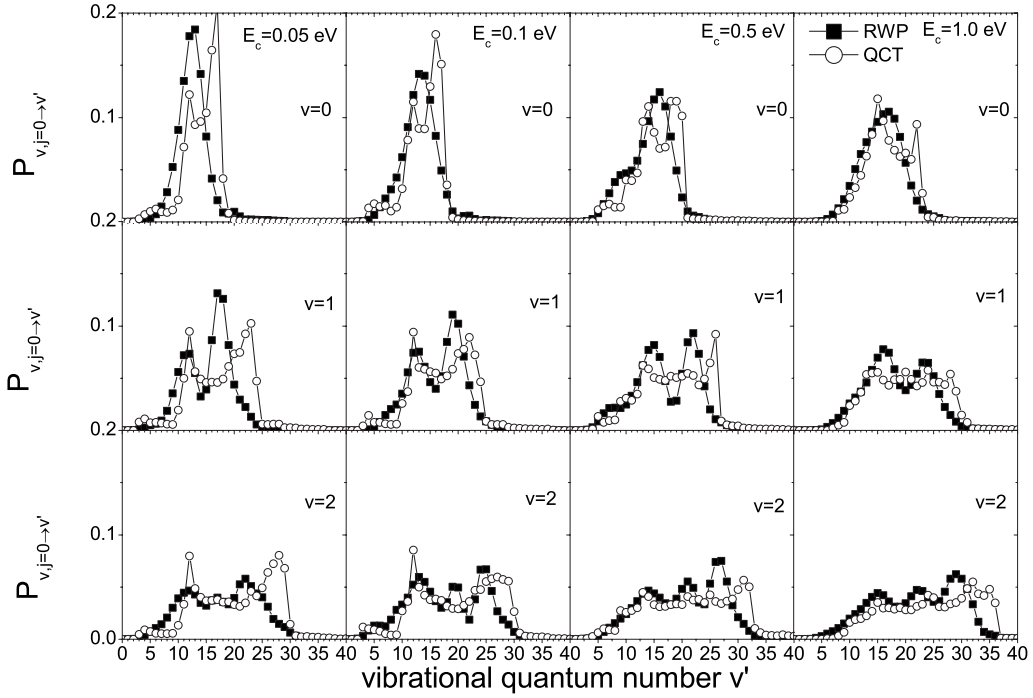

FIG. 4. Final v' state-resolved reaction probabilities at $J=0$ for the C+OH($v=0-2$, $j=0$)→CO(v')+H reactions at selected collision energies (0.05, 0.1, 0.5, 1.0 eV) obtained with the RWP method (black squares) and QCT method (open circles).

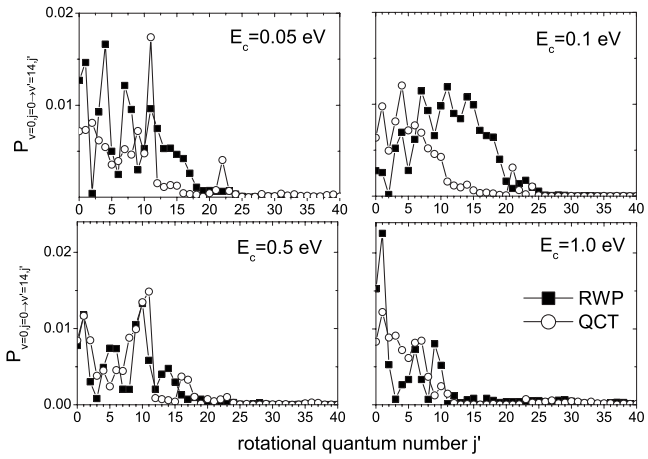

FIG. 5. Final j' state-resolved reaction probabilities at $J=0$ for the C+OH($v=0$, $j=0-5$)→CO($v'=14$, j')+H reactions at selected collision energies (0.05, 0.1, 0.5, 1.0 eV) obtained with the RWP method (black squares) and QCT method (open circles).

tail. An interesting thing to notice is that this structure can be observed only when the rotational energy of the produced CO is low. In the case of a null angular momentum, a very small amount of the total energy is transferred to CO rotation.[3] This implies that the energy is mainly converted in translation and vibration. When looking at the energy distributions, it clearly appears that there are two main peaks in distribution of energy transferred to translation. These two peaks seem to be correlated to the phase of vibration of the OH molecule at the moment when it collides with C. If OH distance is shorter than equilibrium distance, the H atom will be ejected with more energy, leaving less energy to vibration. On the contrary, if OH distance is larger, the H atom will be ejected with less energy and CO will get more vibrational energy. This phenomenon probably also occurs for high angular momenta, but in this case, as part of energy is transferred to rotation, the peaks are somehow averaged and cannot be seen in the global distribution.

Final rotational distributions for a given product vibrational quantum state (we have selected $v'=14$, which is one of the most populated product vibrational state as seen in Fig. 3) at the various collision energies are shown in Fig. 5. The RWP product rotational distributions display a very marked oscillatory behavior, especially for low product rotational quantum states at the lowest collision energy. No clear tendency is observed for the RWP rotational distributions as collision energy increases. In most cases, the distributions peak at low values of j'. The QCT rotational distributions reproduce the overall shape of the RWP distributions with the exception of $E_c=0.1$ eV, for which the QCT distribution is substantially colder.

B. Excitation functions and state-resolved integral cross sections

Figure 6 shows RWP and QCT integral cross sections as a function of collision energy (excitation functions) for the reactions C+OH($v=0$, $j=0-5$)→CO+H and C+OH($v=0-2$, $j=0$)→CO+H. Both RWP and QCT excitation functions do not show energy threshold and the integral cross sections, which are large at low collision energies, substantially decrease as collision energy increases, reaching a constant value at $E_c>0.1$ eV. This behavior, which is characteristic of barrierless exothermic reactions, is similar, among others, to the radical-radical OH+H reaction, as recently reported by Jorfi *et al.*[18] The QCT and RWP excitation func-

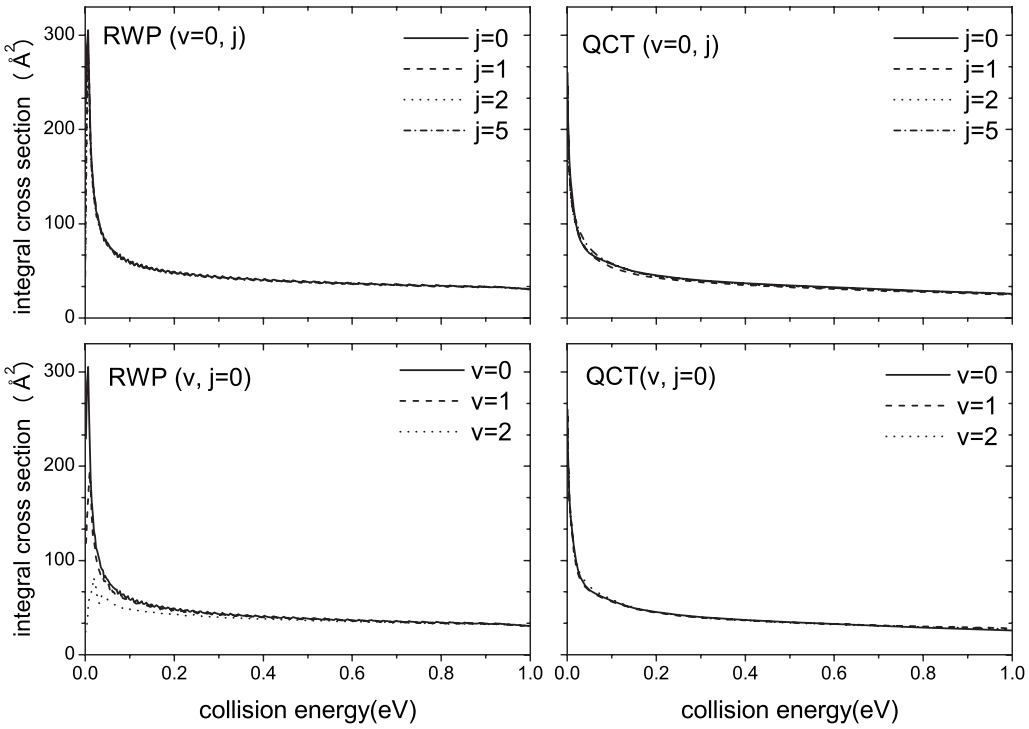

FIG. 6. Integral cross sections as a function of collision energy for the C+OH($v=0-2$, $j=0-5$) reactions calculated by the RWP and QCT methods. Top panels: C+OH($v=0$, $j=0-5$) reactions. Bottom panels: C+OH($v=0-2$, $j=0$) reactions.

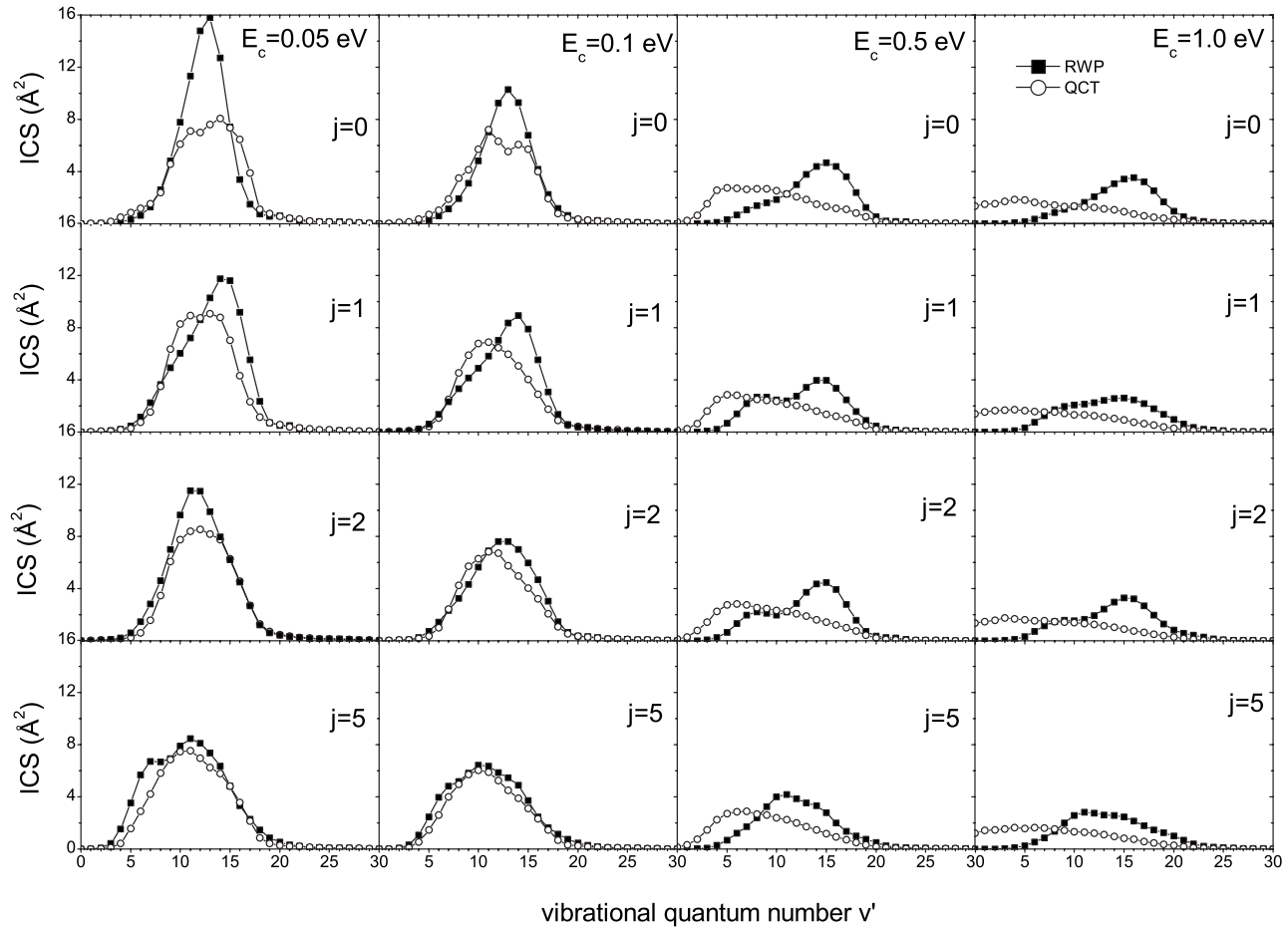

FIG. 7. Final v' state-resolved integral cross sections for the C+OH($v=0$, $j=0-5$)$\rightarrow$CO(v')+H reactions at selected collision energies (0.05, 0.1, 0.5, 1.0 eV) calculated with the RWP method (black squares) and QCT method (open circles).

tions for $v=0$ are not sensitive to the rotational quantum state of OH. The QCT integral cross sections are slightly lower than the RWP ones, especially at low collision energies. The RWP excitation functions calculated for the $v=0-2$, $j=0$ states of OH show a strong dependence on the initial vibrational quantum state below 0.1 eV collision energies. As v increases, reactivity in the low collision energy region decreases substantially, which is in contrast with the corresponding QCT cross sections. This effect is related to the reduction in the RWP reaction probabilities when going from $v=0$ to $v=2$ in the low collision energy region (see Fig. 1). The agreement between the RWP and QCT excitation functions is, however, excellent for collision energies above 0.1 eV.

RWP and QCT vibrationally state-resolved integral cross sections at selected collision energies for the reactions C+OH($v=0$, $j=0-5$)$\rightarrow$CO+H are displayed in Fig. 7. The RWP vibrational distributions peak at high values of v' showing population inversion. As collision energy increases, the RWP distributions become hotter irrespective of the initial rotational quantum number selected. The effect of increasing the initial rotational quantum number is to produce somewhat broader rotational distributions, especially at the lowest collision energies. The agreement between the RWP and QCT vibrational distributions is very good at the 0.05 and 0.1 eV collision energies. However, at the higher collision energies (0.5 and 1.0 eV), the QCT vibrational distributions become substantially colder and broad. As collision energy increases, more and more low vibrational states are populated in the QCT distributions and the peak of the distributions is shifted toward lower v' values. Thus, the agreement between RWP and QCT results is quite satisfactory at low collision energies but becomes substantially worse at higher collision energies. This increase in population of lower v' states as collision energy increases in the QCT vibrational distributions has been observed previously (see Fig. 13 in Ref. 3) and is related to the energy partitioning in the products. As collision energy increases, the fraction of available energy going into rotation increases substantially and this is correlated with a reduction in the fraction of available energy going into vibration.[3] The strong enhancement of the CO rotational excitation with collision energy is attributed to the participation in the reaction of progressively larger orbital angular momenta. This effect is not seen though in the corresponding RWP results. However, the RWP integral cross sections have been obtained by using the $J=0$ reaction probabilities employing a capture model to estimate the $J>0$ reaction probabilities. Although it has been shown that the capture model works really well for this reaction when total integral cross sections are considered, it seems that the model does not work properly for state-resolved quantities at high collision energies.

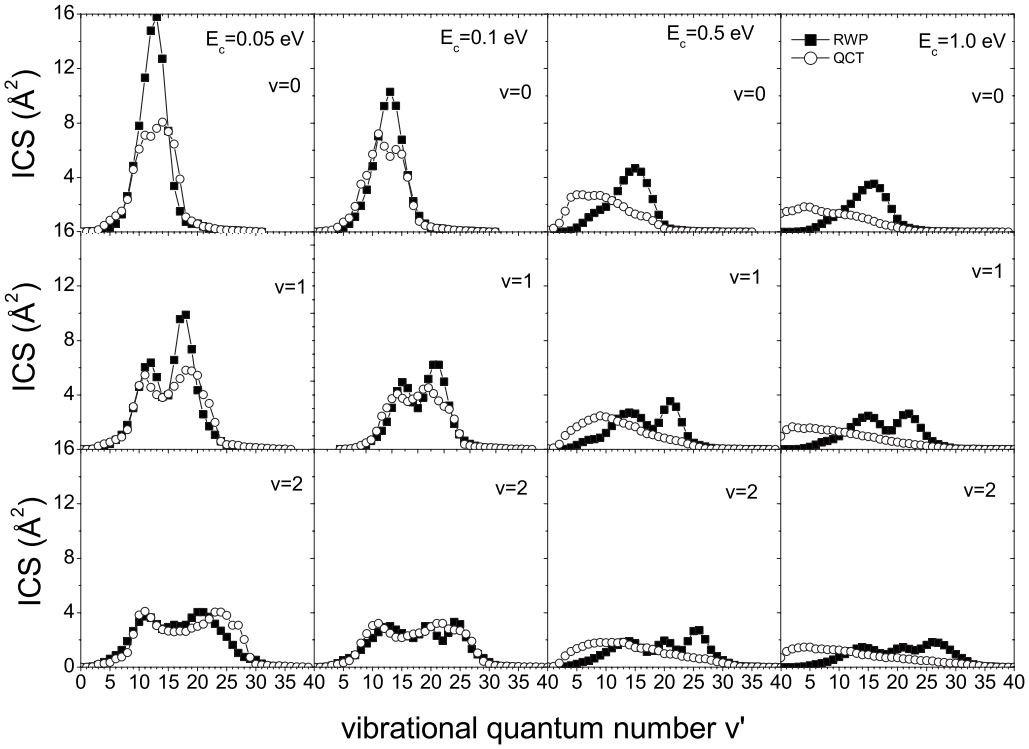

FIG. 8. Final v' state-resolved integral cross sections for the C+OH($v=0-2$, $j=0$)→CO(v')+H reactions at selected collision energies (0.05, 0.1, 0.5, 1.0 eV) calculated with the RWP method (black squares) and QCT method (open circles).

Figure 8 shows RWP and QCT vibrationally state-resolved integral cross sections at the various collision energies in the range 0.05–1.0 eV for the reactions C+OH ($v=0-2$, $j=0$)→CO+H. The RWP and QCT integral cross sections decrease with increasing initial vibrational state, especially at the lowest collision energy. In addition, a clear bimodality appears in both RWP and QCT distributions as initial v increases at the two lowest collision energies. Once again, the agreement between RWP and QCT is excellent at 0.05 and 0.1 eV collision energies, but it gets worse at the two higher collision energies, where the QCT vibrational distributions become increasingly colder in comparison with the lower collision energies, at variance with the RWP calculations.

C. Rate coefficients

We have calculated initial state-selected rate coefficients in a wide range of temperatures up to 500 K for initial rovibrational states ($v=0$, $j=0-5$) of the OH molecule from the corresponding excitation functions using Eqs. (4) and (5). As can be seen in Fig. 9, once the electronic partition function is considered, both RWP and QCT state-selected rate constants first increase at the lowest temperatures up to ≈10 K and then decrease slightly with increasing temperature, reaching a constant value at $T>150$ K. The QCT rate coefficients are slightly lower than the RWP ones in the studied range of temperature. When the RWP rate coefficients are compared with the previous WP results of Lin *et al.*,[4] especially in the low temperature region, the present RWP calculations are in better agreement with the QCT results. The discrepancy between the present RWP rate coefficients and those reported by Lin *et al.* is due to some difficulties in the former WP calculation due to the incomplete damping of the outgoing WP at low collision energies. These difficulties still persist in the present WP calculations at low energies, but here the damping parameters probably work slightly better than in the former WP calculations,[4] at least for $J=0$ (see Fig. 1). The RWP state-selected rate coefficients are slightly dependent on the initial rotational quantum number of the reagent molecule at low temperatures. The agreement found between RWP and QCT rate coefficients is excellent at temperatures above ≈100 K.

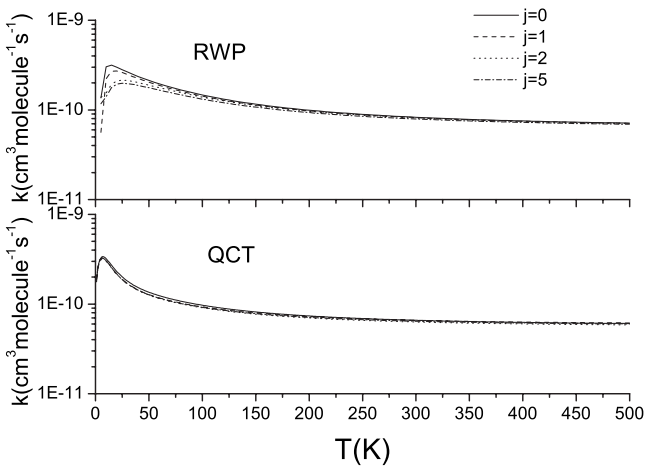

FIG. 9. Rotationally state-specific rate coefficients as a function of temperature for the C+OH($v=0$, $j=0-5$) reaction calculated with the RWP method (top panel) and the QCT method (bottom panel).

IV. CONCLUSIONS

In this study, three-dimensional RWP calculations for the $C(^3P)+OH(X\ ^2\Pi)\rightarrow CO(X\ ^1\Sigma^+)+H(^2S)$ reaction at several initial and final rovibrational states of the reagents and products have been performed for total angular momentum $J=0$. A capture model has been applied to estimate reaction probabilities for $J>0$ and integral cross sections as a function of collision energy and rate coefficients have been calculated from the state-to-state reaction probabilities. The RWP calculations of total and state-to-state observables have been complemented with QCT calculations. In all the calculations, the PES of Zanchet *et al.*[1] has been employed. The state-to-state reaction probabilities are slightly dependent on the collision energy, but the results demonstrate that the dependency on initial rovibrational quantum states of the OH molecule is weak. The calculated RWP and QCT excitation functions decrease with increasing collision energy, as expected for an exothermic barrierless reaction. An overall good agreement between the RWP and QCT reaction probabilities and integral cross sections has been found. Initial v, j state-selected RWP and QCT rate coefficients have been calculated by averaging the corresponding excitation functions over translational energy and considering the electronic partition function for the title reaction. The RWP and QCT state-selected rate coefficients are practically insensitive to temperature, with the exception of the low temperature region, and the agreement found between both RWP and QCT results is quite good.

ACKNOWLEDGMENTS

N.B. thanks S. K. Gray for his guidance. Partial financial support from the Spanish Ministry of Education and Science (Project No. CTQ2008-02578/BQU) is gratefully acknowledged. A.Z., P.H., and B.B.-H. acknowledge support from the Institut du Développement des Ressources en Informatique Scientifique (IDRIS) in Orsay (France), the UTINAM laboratory for its fast cluster, and also the Pôle de Sciences Planétaires of Bourgogne Franche-Comté.

[1] A. Zanchet, B. Bussery-Honvault, and P. Honvault, J. Chem. Phys. A. **110**, 12017 (2006).
[2] A. Zanchet, P. Halvick, J. C. Rayez, B. Bussery-Honvault, and P. Honvault, J. Chem. Phys. **126**, 184308 (2007).
[3] A. Zanchet, P. Halvick, B. Bussery-Honvault, and P. Honvault, J. Chem. Phys. **128**, 204301 (2008).
[4] S. Y. Lin, H. Guo, and P. Honvault, Chem. Phys. Lett. **453**, 140 (2008).
[5] S. K. Gray and G. G. Balint-Kurti, J. Chem. Phys. **108**, 950 (1998).
[6] S. K. Gray, E. M. Goldfield, G. C. Schatz, and G. G. Balint-Kurti, Phys. Chem. Chem. Phys. **1**, 1141 (1999).
[7] G. G. Balint-Kurti, A. I. Gonzalez, E. M. Goldfield, and S. K. Gray, Faraday Discuss. **110**, 169 (1998).
[8] M. Hankel, G. G. Balint-Kurti, and S. K. Gray, Int. J. Quantum Chem. **92**, 205 (2003).
[9] Y. Huang, D. J. Kouri, and D. K. Hoffman, J. Chem. Phys. **101**, 10493 (1994).
[10] Y. Huang, S. S. Iyengar, D. J. Kouri, and D. K. Hoffman, J. Chem. Phys. **105**, 927 (1996).
[11] V. A. Mandelshtam and H. S. Taylor, J. Chem. Phys. **102**, 7390 (1995).
[12] V. A. Mandelshtam and H. S. Taylor, J. Chem. Phys. **103**, 2903 (1995).
[13] G. J. Kroes and D. Neuhauser, J. Chem. Phys. **105**, 8890 (1998).
[14] R. Chen and H. Guo, J. Chem. Phys. **105**, 3569 (1996).
[15] S. C. Althorpe, J. Chem. Phys. **114**, 1601 (2001).
[16] M. Hankel, G. G. Balint-Kurti, and S. K. Gray, J. Chem. Phys. **113**, 9658 (2000).
[17] Ph. Halvick and J.-C. Rayez, Chem. Phys. **131**, 375 (1989).
[18] M. Jorfi, P. Honvault, P. Halvick, S. Y. Lin, and H. Guo, Chem. Phys. Lett. **462**, 53 (2008).